SUPERPLASTICITY IN ULTRA HIGH CARBON STEELS

By

R. MUTHURAJ

DEPARTMENT OF METALLURGICAL ENGINEERING

INDIAN INSTITUTE OF TECHNOLOGY KANPUR

MAY 1986

Certificate

This is to certify that the present investigation "Superplasticity in Ultra High Carbon Steels" has been carried out by Mr. R. Muthuraj under my supervision and that it has not been submitted elsewhere for a degree.

M.L. Vaidya
Professor
Department of Metallurgical Engineering
Indian Institute of Technology
Kanpur

Acknowledgements

I indebitably thank Dr. M.L. Vaidya for having provided a pleasant academic environment through his continuous encouragement, enlightening discussions and extensive suggestions throughout the project work.

Special thanks are due to Dr. G.S. Murty for having given necessary discussions from the early stages of the project.

My sincere thanks to all the members of Faculty especially Dr. R.K. Ray, Dr. R.K. Dube, Dr. S.P. Gupta and others for their kind help during the work.

I also wish to thank the staff members of the laboratories/workshop for providing invaluable help and excellent facility.

I am indebted to all of my friends for all kinds of help and co-operation.

My sincere thanks are due to all the others who really worked for the preparation of this report.

- R. Muthuraj.

ABSTRACT

Ultra high carbon steel containing 1.27% carbon, commercially used for making files has been subjected to various thermo mechanical treatments, such as, (i) cold working-annealing, (ii) thermal cycling between 900°C to 930°C,(iii) hot iso-rolling at 940°C and 740°C, (iv) hot continuous rolling from 880°C to 600°C, and (v) quenching from 930°C followed by hot iso-rolling at 730°C. Samples obtained by the various treatments have been tested at 610°C in tension using differential strain rate tests and constant speed tests to evaluate their stress-strain rate behaviour, strain rate sensitivity values and ductility values. It has been demonstrated that superplastic behaviour can be induced in the ultra high carbon steel by the treatments: (i) hot continuous rolling, (ii) hot iso-rolling at 740°C, (iii) quenching followed by hot iso-rolling. Thermal cycling and cold work-annealing treatments are not so effective in refining the structure and inducing superplasticity. Ductilities exceeding 300% have been obtained in the given steel.

Contents

List of Tables

List of Figures

Chapter I

Introduction

There is a constant need for new materials and new manufacturing techniques that will lead to improved engineering components. There is ever increasing demand for better formability with a low cost production method for manufacturing complex components.

Superplasticity in metallic materials has attracted the attention of scientists and technologists over a number of years. During the past 20 years, the industrial metallurgists in this field have altered their basic questions from "How do we make superplastic alloys" to "How can we make useful superplastic alloys?" to "How does one make useful alloys superplastic?" A large number of superplastic alloys have been discovered but few of them have reached the market place. However much emphasis is still on the research and phenomenology of superplasticity.

The essential requirement for superplastic deformation are fine and stable grain size, typically of the order of less than 10 microns[1] at a high temperature of order of 0.5 T_m where T_m is the absolute melting temperature. The major advantage of superplastic deformation requires low stress with large elongation for high temperature forming and good strength properties at low service temperature.

In the case of ultra high carbon steels (UHC), from a practical and commercial point of view, it would be

highly desirable that UHC steels could be superplastic at normal strain rates 10^{-1} to 1 per second[2] (600 to 6000% per minute). Such a goal is a realistic one and the principal method of achieving it is to develop a grain size finer than one micron in size which remains stable during superplastic flow. Considerable attention has been devoted to superplasticity in steels and a wide range of experimental observations are recorded in scientific literature. Both mechanical and microstructural aspects have been explored in great detail. On the basis of various observations, a number of models have been proposed to account for the experimental observations.

A sound theoretical understanding of the dependence of superplastic strain rate on temperature, grain size and flow stress will be of significant use in optimization of these variable, so that the material can be deformed at the highest possible forming rates and still benefit from the exceptionally large, neck-free elongation associated with superplasticity.

1.1 Superplastic Behaviour

1.1.1 Characteristics of deformation

Under isothermal and constant grain size conditions, during uniaxial testing, this class of materials obey a constitutive equation of the type[3]

$$\sigma_t = K \dot{\varepsilon}_t^m \qquad (1)$$

where σ_t is the applied stress

$\dot{\varepsilon}_t$ is the strain rate, m (the strain rate sensitivity index)

and K is the material constants which critically depend on experimental observations like temperature (T), grain size (L), strain rate etc.

Superplastic deformation is quasi-viscous with a delay time for the onset of steady state flow. The strain necessary to attain the steady state increases with increasing strain rate and decreasing temperature. The transition from the unsteady to steady state flow is gradual. When the stress strain rate relation is evaluated with the steady state most superplastic materials show a sigmoidal variation of ln σ_t with ln $\dot{\varepsilon}_t$ (Figure 1.1a). This plots are divided into three approximately linear regions of different slopes. The strain rate sensitivity index on the other hand, goes through a maximum with strain rate. Region II of Figure 1.1b with m > 0.3 delineates the strain rate range over which superplasticity occurs. So from equation (1) it follows that in this region strain rate increases more slowly with stress compared with regions I and III. However it is clear that beyond a strain rate $\dot{\varepsilon}^*$, m decreases with increasing strain rate. On account of this region beyond a strain rate of $\dot{\varepsilon}_t^*$ must be regarded as the range in which superplasticity is slowly being lost due to competition from less sensitive processes. In region IIa of Figure 1.1b optimal superplastic deformation is obtained. Under these conditions, the flow stress is very small.

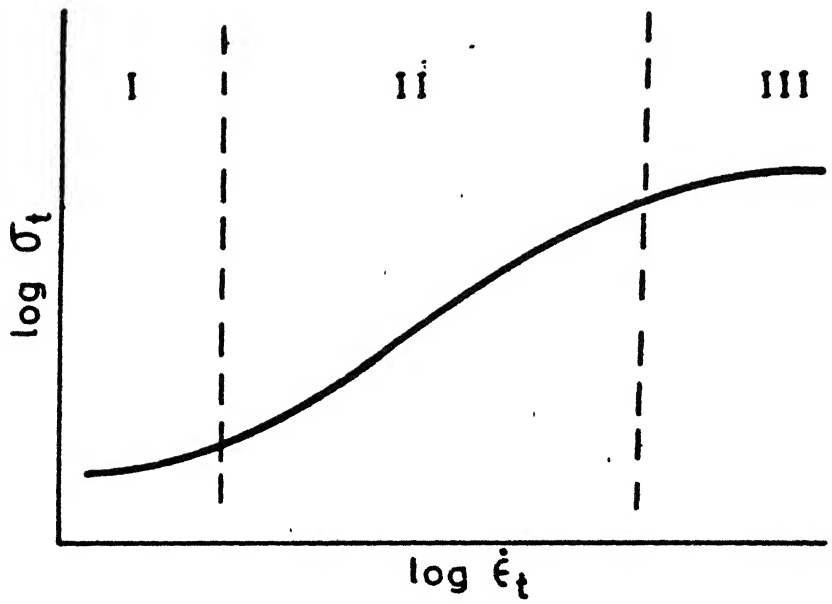

(a)

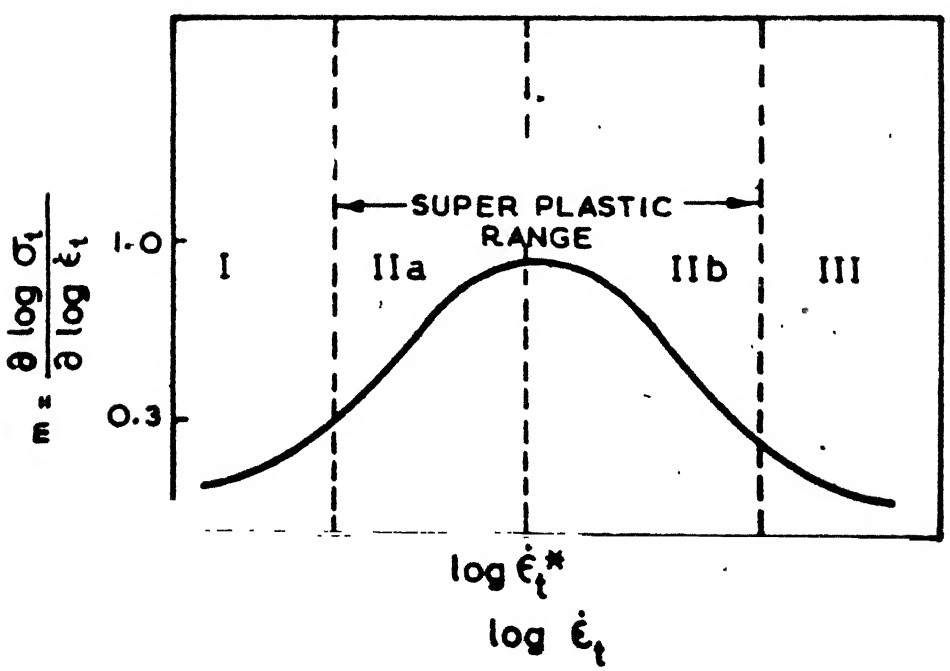

(b)

Figure 3.2 The relationship between (a) stress, σ_t, and strain rate, $\dot{\epsilon}_t$ and
(b) strain-rate sensitivity index, m and strain rate, for superplastic deformation (Schematic)

the flow stress is very small and the material exhibits negligible work hardening.

The sigmoidal ln σ_t - ln $\dot{\varepsilon}_t$ curve is shifted downwards and to the right with decreasing grain size, and/or increasing temperature. Many materials e.g. Sn-Pb eutectic, Mg-Al eutectic, Al-Cu eutectic, Cu-9 Al-4 Fe, exhibit this three stage strain rate behaviour. With some alloys (e.g.) Zn-22 Al, Ni-39 Cr-10 Fe-1.75 Ti the various stages are not well defined, and the stress strain rate curves are essentially linear over a wide range of strain rates.

The steady state strain rate $\dot{\varepsilon}_t$ in the high temperature deformation may be expressed by the equation[4,5]

$$\dot{\varepsilon}_t = \frac{AGb}{kT} \left(\frac{b}{d}\right)^p \left(\frac{\sigma}{G}\right)^n D_o \exp\left(-\frac{Q}{RT}\right) \qquad (2)$$

where A is the dimensional constant, G shear modulus, b Burger's vector, k Boltzman's constant, T the absolute temperature, d the grain size, D_o the frequency factor, Q the activation energy, R the gas constant, $n = \frac{(\ln \dot{\varepsilon})}{(\ln \sigma)}$ stress component and $p = \frac{(\ln \dot{\varepsilon})}{(\ln d)}$ is the grain size exponent. In the literature on superplasticity, the stress exponent (n) is replaced by the strain rate sensitivity parameter $m = \frac{1}{n}$.

The strain rate sensitivity index, m is very important parameter in characterising structural superplastic deformation. This is the slope of ln σ_t - ln $\dot{\varepsilon}_t$ curve. m also varies with temperature and structure (grain size).

1.1.2 Determination of m using strain rate change test

As shown in Figure 1.2 if the cross head velocity is increased from V_1 to V_2 there is a corresponding increase in load from P_B to P_A.[6] If m is assumed to be nearly independent of strain rate in the range covered by the velocity increase, then

$$m = \frac{\ln P_A/P_B}{\ln V_2/V_1} \tag{3}$$

Another approach is to calculate the true stresses and the true strain rate at the points of maximum load, then

$$m = \frac{\ln \sigma_t^A/\sigma_t^B}{\ln \dot{\varepsilon}_t^A/\dot{\varepsilon}_t^B} \tag{4}$$

According to Hedworth and Stowell[7] in the case of Al-Cu eutectic corresponding to two velocity changes by equation (3) yielded values of m = 0.67 and 0.72 while equation (4) gave m = 0.96 and 1.25. The discrepancy was explained by recognising that the strain rate was changing throughout the test. In addition as the maximum in the load extension curve can precede the onset of steady state, work hardening transient effects can also influence the value of m when equation (4) is used.

The strain rate sensitivity is alse determined as the slope of $\sigma_t - \dot{\varepsilon}_t$ curve either graphically or better by using a curve fitting procedure and other methods like stress relaxation tests[8] which involves the plastic deformation to some choosen stress level at which stage, the cross head

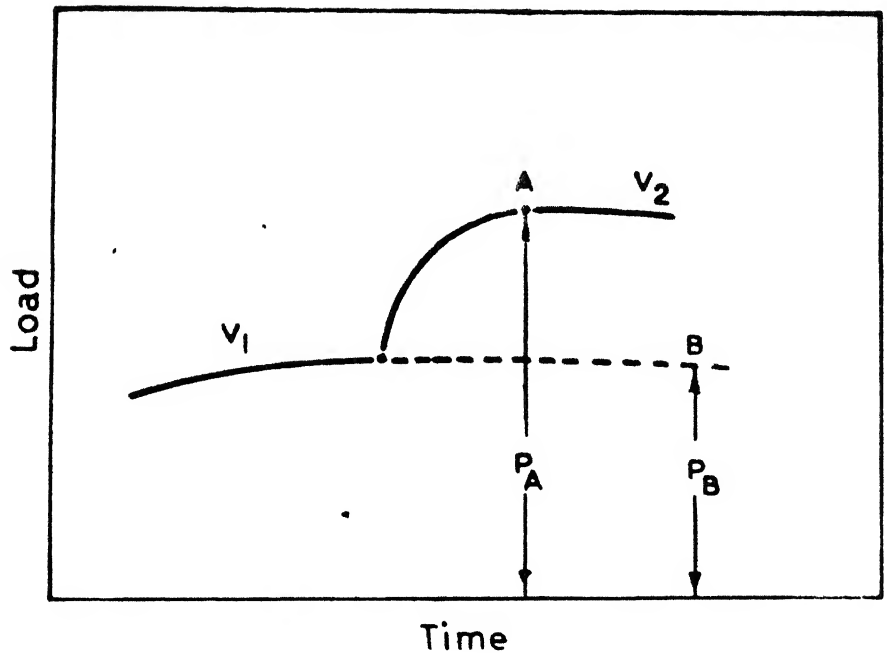

Figure 2.13 A schematic load-time diagram representing a velocity change from V_1 to V_2. Times A and B represent the same strain at the different pulling speeds (Backofen, Turner and Avery (12))

$$m = \frac{\ln (P_A / P_B)}{\ln (V_2 / V_1)} \qquad .. \quad 2.31$$

movement is stopped and a continuous decrease in stress is observed as a function of time, t. The peak m values obtained by the method as the slope of $\sigma_t - \dot{\varepsilon}_t$ curve are greater than those calculated from a change in strain rate tests. The change in strain rate test and stress relaxation method often give similar values of m.

1.2 Necessary Conditions

The existence of fine grained less than 10 micron equiaxed polyphase structures, with the phases displaying similar ductility at the temperature of deformation, is conductive to superplasticity. The rates of deformation should be as to give m values 0.3 or more.

Only Duplex and multiphase structures have stable grain sizes which are resistant to grain growth and those alloys are significantly more superplastic. The types of phases, their distribution, the grain boundary condition, temperature, strain rate and grain size all influence the degree of superplasticity observed. If the strain rate is set to match the velocity of diffusion processes, then most pronounced superplastic effects are observed. When the grain size is coarse, or the grain boundaries are not flat and the structure is not equiaxed and uniformly fine grained no superplastic effects can be seen.[9] Non-deformable second phase particles, as found in dispersion hardening alloys, eliminated the effect of fine grain size and led to cavitation.[10] In iron-carbon alloys[11] undissolved carbides, residual massive martensite and non-equilibrium

structures have been shown to prevent superplasticity. Moreover, when the condition $0.4\ T_m \leq T < T_m$ where T is the absolute temperature of superplastic deformation and T_m is the appropriate transformation temperature (on the absolute scale) which defines the upper limit of two phase field for the alloy, is not satisfied or when grain growth at the temperature of deformation is very rapid, significant superplasticity is absent. When one phases is high melting and or proportion of the second phase is very small, optimal superplasticity is not observed.

Cast or cast and homogenised alloys of eutectic or polyphase compositions are also not superplastic although in wrought condition, they exhibit significant superplasticity. This difference has been attributed variously to the lamellar, dendritic or interlocking nature of grain boundaries in the cast alloys. Superplasticity is seen in coarse grained materials that contain a fine stable subgrain network. Thus the macroscopic features described form a set of necessary but not sufficient conditions so far as optimal structural superplasticity is concerned.

1.3 Production of Ultrafine Grain Size

Grain growth in pure metals and solid solutions is reasonably well understood. A better situation exists in the case of metals of commercial purity which can be severely worked to produce fine grain size whichare reasonably stabilised by randomly dispersed impurity particles located

predominantly at grain boundaries.[12] When the alloy contains second phase particles, the grain boundary area is eliminated where the boundary intersects the particles and this leads to a decrease in grain boundary energy. When this decrease is more than the reduction in the overall energy of the system resulting from grain growth, there will be no driving force for boundary movement.

For a spherical grains, the maximum grain size that can be developed at a fixed temperature is given by the appropriate expression (4R/3f) (3) where R is the initial particle radius and f is the volume fraction of a second phase. It follows that the second phase particles should be finer when their volume fraction is smaller. However as the temperature of superplastic deformation are usually of the order of 0.5 T_m or more considerable coarsening of the particle is likely. Thus only fine particles that coarsen very slowly should be employed.

In the ideal case, particle size distribution should be bimodal with the large particles (or particles that are far apart) promoting nucleation during recrystallisation and the smaller particles ensuring a small fine grain size. Nucleation rate during recrystallization, on the other hand is increased by heavy working at high strain rates (e.g.) rolling, extrusion. A solution treatment precedes and a cold rolling procedure, follows hot rolling is also used to refine the grain size. Mere cold work, without intermediate hot rolling is less effective. In the case of low carbon[9]

as well as low alloy steels by adding appropriate combinations of α and γ stabilisers and hot working the alloy steels[13] duplex structures that give rise to superplastic properties at optimal temperatures could be generated (e.g.) Aluminium addition to low C steels; molybdenum and titanium addition to iron-4% nickel. In low alloy steels[14] on the other hand controlled thermal cycling leads to a fine grained microstructure. The Powder Metallurgy route[15] has advantages particularly when the compositional variations can cause difficulties. For instance, conventionally formed nickel-base super alloys segregation and banding are severe problems.

1.4 Methods of Grain Refinement

Several methods are available for grain refinement, starting from casting by rapid solidification, thermal cycling, thermomechanical processing etc., including phase transformation, recrystallisation, working of duplex alloys and phase separation in duplex alloys. In phase transformation and recrystallisation method, the aim is to nucleate several product (transformed or recrystallised) grains within each grain of parent microstructure. In deformation of duplex alloys, grains of two phases are broken up and spheroidised. In phase separation of duplex alloys, the starting microstructure is usually either martensitic or a supersaturated solid solution. Phase separation of non-equilibrium structure into two equilibrium phases can produce a fine grain Duplex microstructure. Often, combinations of the methods of grain

refinement are employed together. Schematic diagram of all the above is given in Figure 1.3.

1.4.1 Grain refinement by phase transformation

The ferrite-austenite phase transformation has been used for grain refinement in steels. Several studies[16] have shown that cycling repeatedly through the transformation temperature results in very fine grain sizes. The mechanism of grain refinement in this case is the nucleation of the product phase at grain boundaries, in the parent phase. As the grain size becomes finer during successive cycles, more nucleation sites are available for the next transformation. Eventually at submicrometer grain sizes, the grain size saturates and further cycling does not produce additional grain refinement.

In recent years, controlled rolling process[17] has been developed to produce fine grain sizes in high strength low alloy steels. It can be done as a continuous process unlike thermal cycling; thus controlled rolling is more suitable for large-scale production. The key to grain refinement by controlled rolling is transformation to ferrite of hot worked, unrecrystallised austenite. The austenite is prevented from recrystallising by Niobium and Vanadium carbonitrides that precipitate in the austenite during hot working. The heavily deformed austenite provides a high density of nucleation sites for ferrite grains and the transformed ferrite grain size is extremely fine.

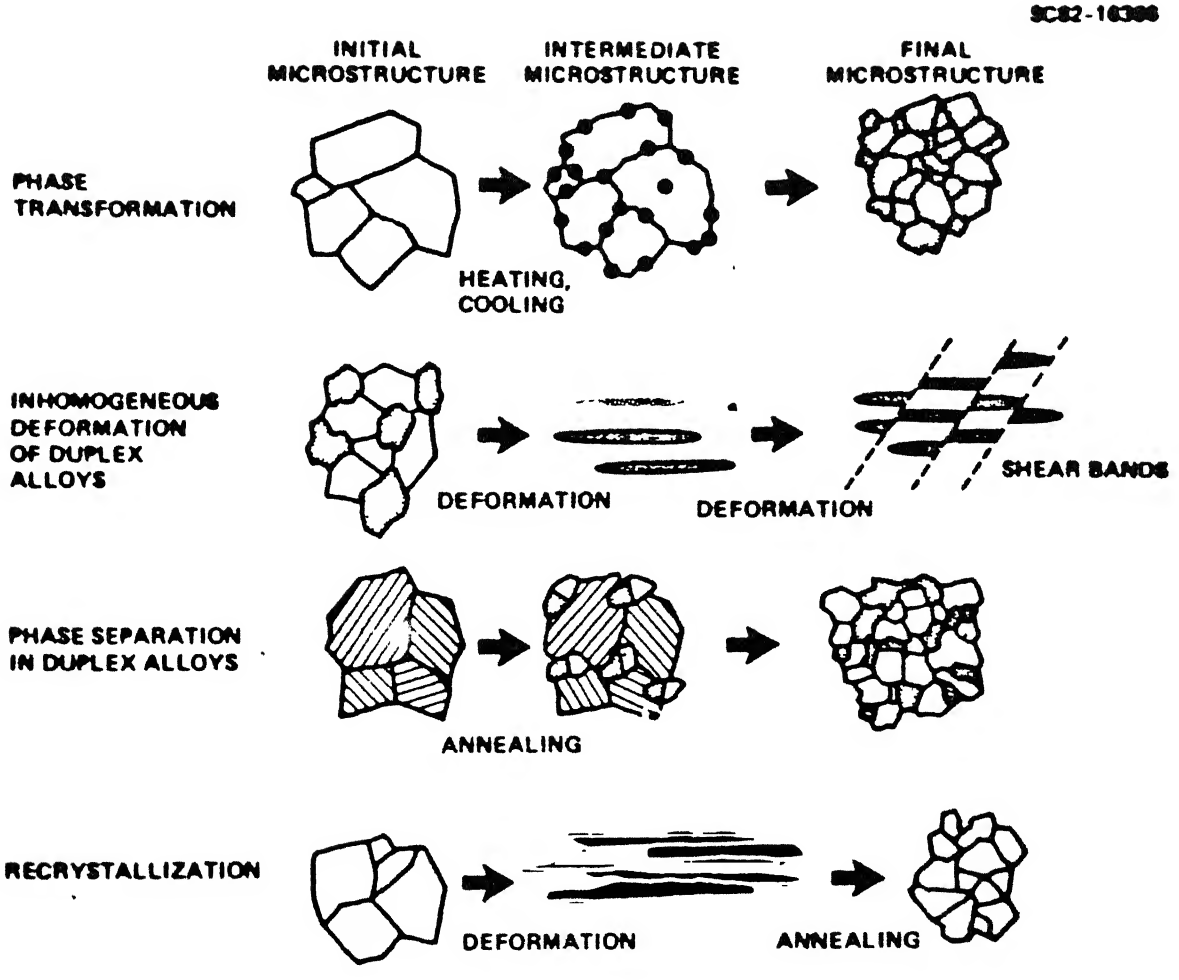

Figure 2 - Schematic showing the general mechanisms of grain refinement.

1.4.2 Grain refinement by deformation of duplex alloys

Many superplastic alloys are duplex alloys, that contain two deformable phases, like titanium alloys, zirconium alloys, hypereutectoid steels,[18,19] Zn-Al alloys, α/β brasses, Pb-Sn alloys, Al-Cu, Al-Ni alloys. Grain refinement of duplex alloys can be by two methods; deformation of equilibrium duplex microstructures and recrystallisation in non-equilibrium microstructures.

Grain refinement of duplex alloys that already have a duplex equilibrium microstructure is accomplished by extensive deformation (rolling or extrusion are commonly used) near the temperature range where superplasticity are observed. An annealing treatment is frequently used after deformation, although dynamic recrystallisation generally occurs during deformation.

However recrystallisation alone cannot produce a finer, intermixed, two phase microstructure. Homogeneous deformation of a duplex structure will produce elongated phase regions, perhaps recrystallised so that each original grain contains several recrystallised grains, but the phases will not be intermixed, because they have different chemical compositions. The key to grain refinement of alloys that already have a duplex microstructure is inhomogeneous deformation. Elongated phase regions are indeed broken-up during deformation through the inhomogeneous nature of deformation process. Annealing permits recrystallisation of each phase and allows sufficient diffusion for spheroidisation to the

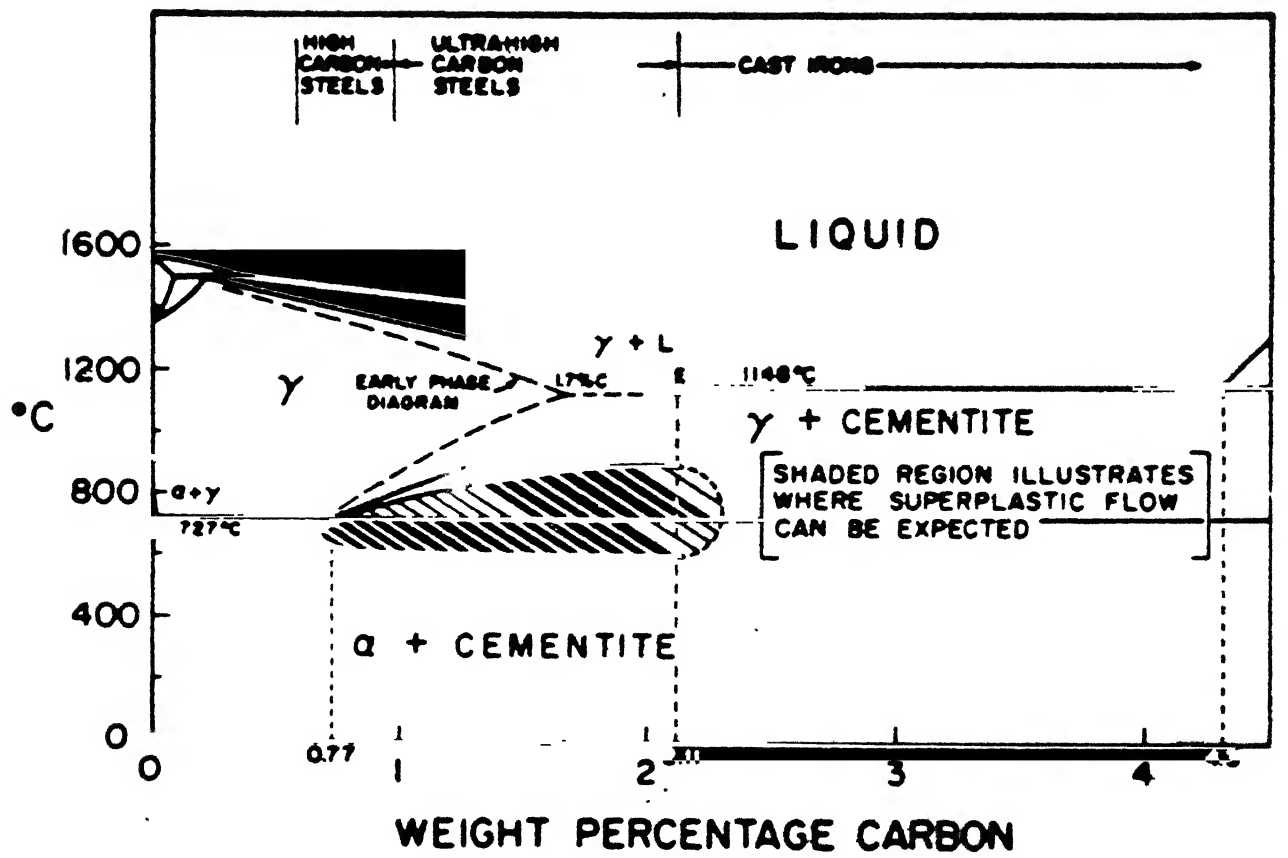

Fig. I.4. Fe-C phase diagram showing composition and temperature range for superplasticity in ultra-high carbon steels (Ref. 10).

desired equiaxed fine grain structure. In this case where heavy deformation is not used, the original elongated grains are not sufficiently distorted, and recrystallisation does not produce the equiaxed, duplex microstructure require for superplasticity.

1.4.3 Grain refinement by phase separation

Annealing duplex alloys, with a non-equilibrium microstructure causes phase separation into two equilibrium phases. Separation of the initial microstructure into two equilibrium phases can produce a fine grain duplex microstructure.[20] A fine grain size is obtained if a high density of nuclei of the two phases form in the starting non-equilibrium microstructure. Substantial diffusion is required to attain the equilibrium duplex phase mixture; the amount of diffusion depends on the chemical composition of the equilibrium phases and the density of nucleation sites.

The non-equilibrium starting microstructure is usually martensitic or a quenched solid solution. The substructure present in martensitic microstructures frequently provides a high density of nucleation sites for the equilibrium phases. Warm deformation of quenched solid solutions prior to phase separation can be used to enhance grain refinement during phase separation. In titanium alloys[20] the starting microstructure is martensitic, obtained by quenching the alloys from the β phase field. Annealing in the $\alpha + \beta$ two phase field causes the martensite to separate

into α and β equilibrium phases. The extent of grain refinement depends on the annealing conditions, which controls the rate of nucleation and growth of equilibrium phases.

Another grain refinement by phase separation is the spinodal decomposition reaction in 78% Zn-22% Al.[21] Above room temperature, the monotectoid alloys transform by the classic eutectoid decomposition route into a lamellar microstructure with poor superplastic properties. Near room temperature, where the decomposition occurs slowly, a spinodal decomposition reaction occurs, producing a duplex microstructure of two equilibrium phases. The spinodal decomposition reaction occurs rapidly in the binary alloy and the coherency between two phases is quickly lost. The resulting microstructure has been termed granular, which exhibits extensive superplasticity.

1.4.4 Grain refinement by recrystallisation

Recrystallisation[22] is a universal technique for grain refinement. Particle effects on recrystallisation fall into two categories:

1. Small particles ($d < 1\ \mu m$) supress nucleation and retard growth of recrystallising grains by exerting a drag force on dislocation cell walls and subgrain boundaries.
2. Large particles (diameter $> 1\ \mu m$) create nucleation sites for the recrystallised grains. During deformation, a deformation zone forms around the non-deformable particles nucleation of recrystallised grain occurs within the deformation zone.

Two modes of recrystallisation can be used both rely on particles to produce fine grain size. The discontinuous recrystallisation mode occurs by nucleation and growth of recrystallised grains. The key factor in this case is formation of a high density of nucleation sites like larger particles for recrystallising grains. This has been successful in various precipitation hardening Al-alloys.

Continuous recrystallisation is the alternate recrystallisation mode available for grain refinement. Sometimes termed recovery or insitu recrystallisation, continuous recrystallisation proceeds by subgrain coarsening until high angle boundaries appear and the structure is recrystallised. Nucleation of individual recrystallised grains does not occur in continuous recrystallisation. Supression of discontinuous recrystallisation is essential to obtain continuous recrystallisation, with high densities of small particles.

1.5 Grain Coarsening Control

In addition to starting with a fine grain size, grain growth must be suppressed during the slow superplastic forming processes at elevated temperature. Two general methods are available for grain size are: the pinning force excerted on boundaries by solute atoms and particles and the alloying element partitioning that occurs in duplex alloys. Particles restrict grain growth by exerting a drag force on migrating boundaries by the reduction of grain boundary energy that occurs when the boundary intersects the particle. All

classes of superplastic alloys except duplex alloys employ particles for grain size control. Restraint of grain growth by solute atom drag force is thought to be insignificant compared to the effect of particles.

In duplex alloys, grain growth is restricted by partitioning of alloying elements between the two phases. Grain coarsening occurs initially by elimination of many $\alpha - \alpha$ grain boundaries and $\beta - \beta$ boundaries, leaving unconnected grains of each phase. For further grain growth, diffusion is required. Partitioning of alloying elements in a duplex microstructure, necessiates substantial diffusion for the isolated grains of each phase to coarsen.

1.6 Mechanisms of Steady State Flow

Several reviewers[23,24,25] have summarised the various mechanisms of superplasticity. Microscopic evidence indicate some intergranular dislocation activity in the superplastic region II, but the dominant deformation mechanism appears to be the grain boundary sliding.

The contribution from grain boundary sliding decreases in region I. Several mechanisms have been developed theoretically to explain superplastic processes, but, without exception, each model is inconsistent with one or more of the established experimental trends. The theories proposed for region II, can be broadly divided into

a) Diffusional flow mechanisms,

b) Dislocation creep theories, and

c) Grain boundary deformation models.

1.6.1 Diffusional flow mechanisms

It is now well recognised that pure diffusional flow (N-H and coble creep mechanisms) is inadequate in giving rise to large plastic strain in polycrystalline materials other than bamboo-type grain structures. Ashby and Verall[26] developed a theory based on grain boundary sliding with diffusional accommodation through the lattice as well as grain boundaries.

A group of four regular hexagonal grains in a two dimensional model is considered. These grains through a neighbouring switching event move from the initial state to a final one with an identical grain shape. In this process, the grains undergo accommodation strains and translate past each other by grain boundary sliding. This gives atrue strain of 0.55 as a result of this switching event. A constitutive equation based on the mechanism is derived and it is similar to the classical Nabarro-Herring-Coble equation for deformation and strain rates that are an order of magnitude faster. Because of the threshold stress, this mechanism predicts a sigmoidal relationship between stress and strain rate.

1.6.2 Dislocation creep theories

These theories are based on grain boundary sliding with accommodation by dislocation motion. According to Ball and Hutchison,[27] a group of grains slides as a unit along some common direction. A grain, which does not have its boundary along the common sliding direction, and is across the sliding path of the group, acts as an obstacle to the sliding process. This leads to stress concentration resulting in emission of dislocations from triple points of blocking grain and the dislocations move to the opposite boundary until the back stress prevents further activation of the source and sliding stops. The leading dislocation in the pile up then climbs into and along the grain boundary. This results in further sliding at a rate governed by the kinetics of deformation climb along grain boundaries to annihilation sites.

1.6.3 Grain boundary deformation models

These models essentially have core mantle approach. The role of grain boundary sliding and other creep mechanisms are coupled to develop these models based on the division of grains into their central "cores" and peripheral "mantles". Grain boundary sliding and its accommodation are limited to the mantle. According to Gifkins[28] the σ^2 term could arise from grain boundary dislocations piled up against a triple point. Gittus[29,30] has combined elements of other theories[31,28] with the suggestion that superdislocations

must move in interphase boundaries to maintain alloy phase structure. Padmanabhan's theory is derived from Ke's model[33] in which the plastic flow occurs by the shearing of groups of atoms in the boundary plane, so that there is interchange of atoms and vacancies leading to a liquid like Newtonian viscous flow.

1.7 Objective of the Present Study

From the literature survey, related to the superplastic behaviour in hypereutectoid steels, the fine grain size is produced from the casting structures mainly through thermal cycling and thermomechanical processing routes, and the test results are reported for the higher temperatures above 0.5 T_m using low strain rates. Though the superplasticity is expected in high carbon steel in the range indicated by the Figure1.4 from 500° to 800°C, at higher temperatures, dynamic grain growth can occur more rapidly through recrystallisation and abnormal grain growth by secondary recrystallisation, grains can grow longer than the critical size and thereby reduction in plasticity.

In the present study, the wrought high carbon steel, used for making files has been investigated for superplastic flow made by different processing routes like thermal cycling, thermomechanical processing routes and a new technique of single quenching and isorolling, and are tested at relatively low temperature at a higher strain rates, to find out the best method of inducing superplasticity in ultra high carbon steels.

Chapter II

Experimental Procedure

2.1 Composition of the Steel

In the present investigation, the high carbon steel used for making files were taken.

The composition was as follows:

Carbon	-	1.27%
Manganese	-	0.26%
Silicon	-	0.25%
Chromium	-	0.66%

2.2 Mechanical Working Process and Various Routes

The wrought steel bars of initial cross section of 3/4" square were cut into 1" length and processed by cold rolling, hot rolling at high strain rates of order of 1 to 10/sec. Different deformation routes were followed.

2.2.1 Hot iso-rolling process

(a) The 3/4" bars were heated to 940°C in the muffle furnace and isothermally hot rolled to a total reduction of 91% to the final thickness of 0.060" with various reduction at each pass.

(b) The bars of initial thickness 0.450" were isothermally rolled at 750°C to a total reduction of 85.5%.

2.2.2 Hot continuous rolling

(a) The 3/4" cut pieces were soaked at 900°C and continuously rolled to about 600°C to a final thickness of 0.070" to a total reduction of 91%.

(b) The same rolling was done at the initial starting temperature of 880°C with 80% total reduction for another sample of initial thickness 0.700".

(c) It is repeated from 880°C to 600°C continuous rolling to a total reduction of 92% with the 3/4" starting cross section to a final thickness of 0.070".

After each rolling operations, the strips were allowed to cool in air to room temperature from the rolling temperature of about 600°C. Before each pass the samples were soaked enough to reach the starting rolling temperature. The temperature of the samples before rolling were measured by the external thermocouple, whereas the finishing temperature was judged by the colour of the hot rolled strip for about 600°C.

2.2.3 Single quench followed by iso-rolling

(a) The sample with initial thickness of 0.370" was heated to 900°C and quenched in water. Then it again heated to 700°C and iso-rolled to a total reduction of 83.8% with various reductions at each pass to a final thickness of 0.060".

(b) The same procedure was done with same initial thickness heated to 920°C, quenched in water and isothermally rolled at 700°C to 85% total reduction with increasing

reductions at each pass to a final thickness of 0.055".

(c) The sample with initial thickness of 0.280" was heated to 900°C, quenched in oil and iso-rolled at 700°C to a total reduction of 78.5% with various reductions at each pass to a final thickness of 0.055".

(d) The same procedure was adopted with initial thickness of 0.380" heated to 900°C, quenched in oil and isothermally rolled at 700°C to a total reduction of 82.4% with various reductions at each pass.

(e) The bar with initial thickness of 0.787" was heated just above the austenising temperature of 940°C and quenched in oil. Then it was heated to 725°C and iso-rolled to a total reduction of 91% with increasing reductions at each pass to a final thickness of 0.072".

2.2.4 Thermal cycling

Thin and long samples were cut from the bar for thermal cycling study. The samples were heated in the tubular furnace to 910°C and quenched in oil and then repeated above and below the transformation temperature for different cycles like 4, 6, 8, 11 and 13 with water quenching. Microstructures had been studied at each stage. Samples had been tried by varying the heating rate and lower the temperature to which it was heated by 10°C at each cycle. After completion of the required cycle it was annealed at 650°C.

2.2.5 Cold rolling and annealing cycle

The 3/4" cut bars were cold rolled to a maximum of 35% reduction at first pass and process annealed at 650°C. This was repeated with 20% reduction at each pass and recrystallised to a cycle of 6 to 8 times at various reductions. Finally it was annealed at 650°C.

The Table 2.1 shows the summary of all treatments given with number.

2.3 Mechanical Testing

All the tests were done on a floor model Instron Universal Testing machine. Tensile coupons were cut along the rolling direction from each strips processed by the above mentioned routes in the form of flat samples with the dimensions indicated by Figure 2.1. True stress, true strain rate were calculated from the load-time record during deformation, assuming uniform deformation along the gauge length. The temperature of the testing was controlled by the furnace fitted with the instrument and monitored throughout the test by the additional thermocouple fitted in the middle of the sample.

The grips for the flat samples with no possibility of slippage of sample during loading were used. Tensile tests were carried out at a constant temperature of 612°C (885°K) controlled by a three zone heating coil furnace with a accuracy of ± 2°C.

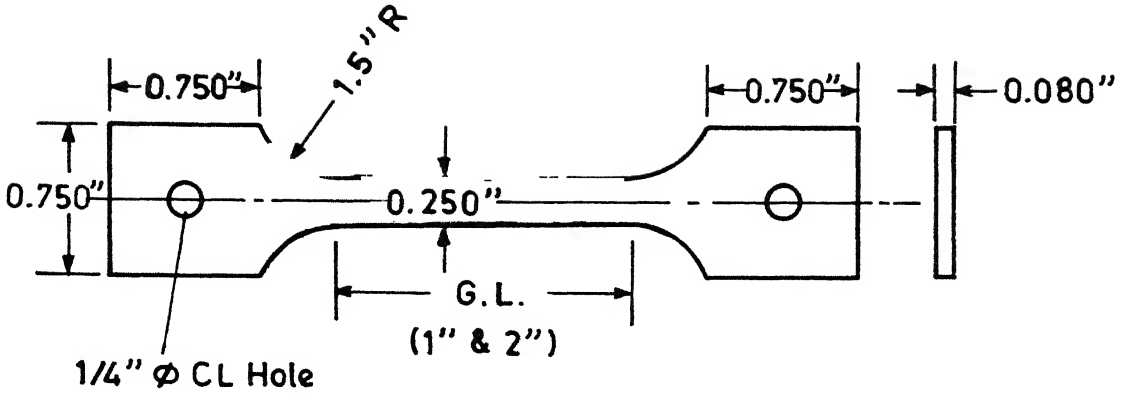

Fig. 2.1 Tensile sample (Flat)

Table 2.1

	Treatment	Temperature range	Total reduction	Sample number
I	Hot iso-rolling process	a) 940°C hot rolling	91%	1
		b) 750°C hot rolling	85.5%	2
II	Hot continuous rolling	a) 900°-600°C hot rolling	91%	3
		b) 880°-600°C hot rolling	80%	4
		c) 880°-600°C hot rolling	91%	5
III	Single quench and iso-rolling	a) 900°C/water quench and isoroll at 700°C	83.8%	6
		b) 920°C/water quench and isoroll at 700°C	85%	7
		c) 900°C/oil quench and isoroll at 700°C	78%	8
		d) 900°C/oil quench and isoroll at 700°C	82%	9
		e) 940°C/oil quench and isoroll at 725°C	91%	10
IV	Thermal cycling	6 times	0%	11
V	Cold rolling and annealing cycle	6 times	77%	12

All the calculations for the instant area of cross section, true stress, true strain rate etc. are done in computer and the model programme and results are shown in Appendix.

2.3.1 Differential strain rate test

Differential strain rate method was adopted to obtain stress-strain rate data of different specimens, starting with the lowest cross speed of 0.02 mm/min, the speed was successively increased to next higher level upto the maximum speed of 5 mm/min. The load corresponding to each of the cross head speeds was thus recorded, from the true stress versus true strain rate data was calculated. In order to minimise the strain effects, the total strain accumulated in one cycle covering the whole range of cross head speeds was kept to a minimum level.

The strain rate sensitivity index "m" was calculated as the slope of $\log \sigma_T - \log \varepsilon_T$ plot or in some cases from the relation

$$m = \frac{\log P_2/P_1}{\log V_2/V_1}$$

where P_1 and P_2 are the steady state loads corresponding to cross head speeds V_1 and V_2 respectively.

2.3.2 Combination test

The samples with gauge length of 50 mm were used only for differential strain rate test. The samples with 25 mm

gauge length were used for differential strain rate test in combination with constant cross head speed test. At some interval the differential strain rate test was carried out to check for the steady state.

2.4 Metallography

The samples cut from each strip processed above were cold mounted using Araldite. The usual polishing procedure starting from belt grinder to series of emery paper and cloth polishing by Alumina powder. Both the longitudinal and transverse directions were studied.

The etchant used was prepared with 5 ml nitric acid with 4 grams of picric acid dissolved in methyl alcohol to make 100 ml, to reveal ferrite boundaries to differentiate ferrite from martensite or carbides especially in the case of spheroidised structures. It was etched for 10 to 15 seconds and etched for longer time for the clarity of grain boundaries. As the grain size was very fine, no distinction was made between interphase boundaries and grain boundaries in estimation of grain size.

2.5 SEM

The particle size distribution were studied in early stages using scanning electron microscope at higher magnifications of 5000X, for different treatments. The fractured samples were also studied in the low magnification to find out the fracture structure and mode of failure whether it is brittle or ductile.

Chapter III

Experimental Results

The results of the experiments performed according to procedures explained in the previous chapter are presented below. The order in which the results are presented is:

1. Microstructures obtained by various thermal and thermomechanical treatments.
2. Stress versus Strain rate data for samples treated differently.
3. Strain rate sensitivity versus Strain rate data for various samples.

3.1 Microstructures

(a) As received condition of the steel: Figure 3.1. The features to be noted are:

- Large grain size (~50 μm)
- Grain boundary network of cementite
- Lamellar pearlite within grains.

(b) After thermal cycling treatment: Figure 3.2. The features to be noted are:

- Fine grain structure (~2 μm)
- No grain boundary network of cementite
- Fine globular cementite
- Patches of lamellar pearlite.

(c) After cold work - anneal treatment: Figure 3.3. The features to be noted are:

Fig. 3.1 Microstructure of initial grain size 500X

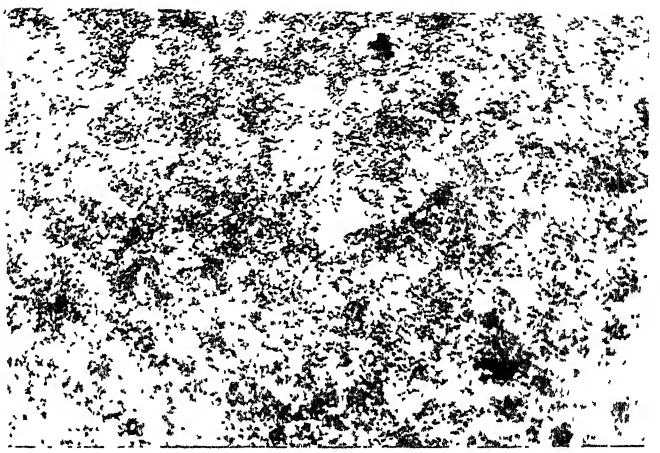

Fig. 3.2 Microstructure of thermally cycled (6 times) sample 1000X

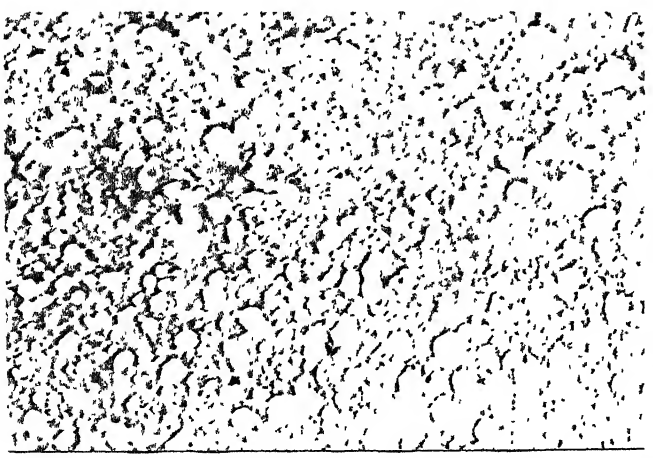

Fig. 3.3a Scanning micrograph of cold work and annealed sample 1000X

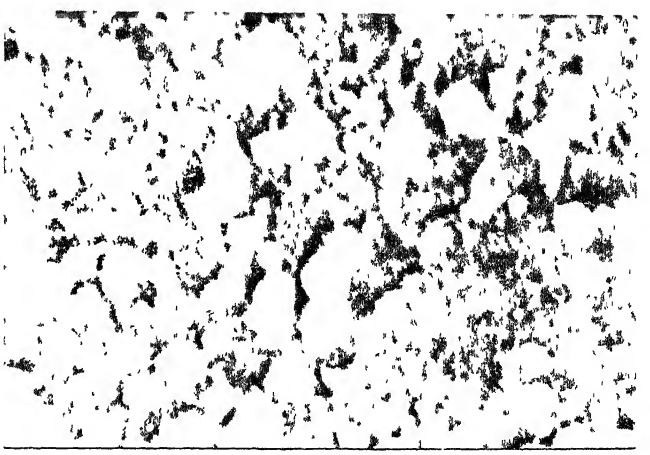

Fig. 3.3b Same as 2500X showing the nonuniform size distribution of cementite particle

the finest and the most equiaxed microstructure. The degree of structural refinement achieved by hot continuous rolling is almost equivalent to that by the earlier treatment, viz. quenching followed by iso-rolling. Cold rolling followed by annealing is not very effective in refining the cementite phase. Also the ferrite (matrix) grains are coarser than those obtained by hot iso-rolling or continuous rolling. Thermal cycling does refine the cementite phase and the grain size but to a much lesser extent. It is unable to spheroidise the cementite in pearlite.

3.2 Stress-Strain Rate Behaviour

The data obtained in the differential strain rate tests for various samples is presented in Figure 3.8 as log-log plots. The flow stress for plastic deformation, at 610°C, appears to increase with increasing strain rate in all cases. The nature of curves is sigmoidal, i.e. the slope changes from a low value at low strain rates to a higher value at the intermediate strain rates and again decreases to a lower value at high strain rates.

As far as the flow stress levels are concerned each sample shows a different level. The samples subjected to thermal cycling treatment show the highest level of flow stress value at a given strain rate. It is followed by the samples treated by quenching and subsequently hot iso-rolled. The cold worked and annealed samples show the highest flow stress levels at lower strain rates. Similarly the samples hot isorolled at 940°C show higher flow stress levels.

- Fine grain structure (~5 μm)
- Coarse globular cementite
- No cementite network or patchy pearlite.

(d) After hot iso rolling:

(i) Hot iso rolling in the austenite range: Figure 3.4. The features to be noted are

- Elongated grains, coarse grain structure
- Globular cementite in banded form

(ii) Hot isorolling at 750°C: Figure 3.5. The features to be noted are:

- Fine grain structure (~ 2 μm)
- Fine globular cementite; not well dispersed
- No cementite network or lamellar pearlite.

(e) After hot continuous rolling: Figure 3.6. The features to be noted are:

- Extremely fine grained structure (~ 0.5 μm)
- Very fine globular cementite; well dispersed
- Slight directionality to the structure along rolling direction.

(f) After single quench followed by iso-rolling: Figure 3.7. The features to be noted are:

- Extremely fine grained structure (~0.5 μm)
- Very fine globular cementite; well dispersed
- No directionality to the structure (equiaxed).

3.1.1 Remarks

As far as the microstructural development is concerned single quench followed by iso-rolling around 700-725°C gives

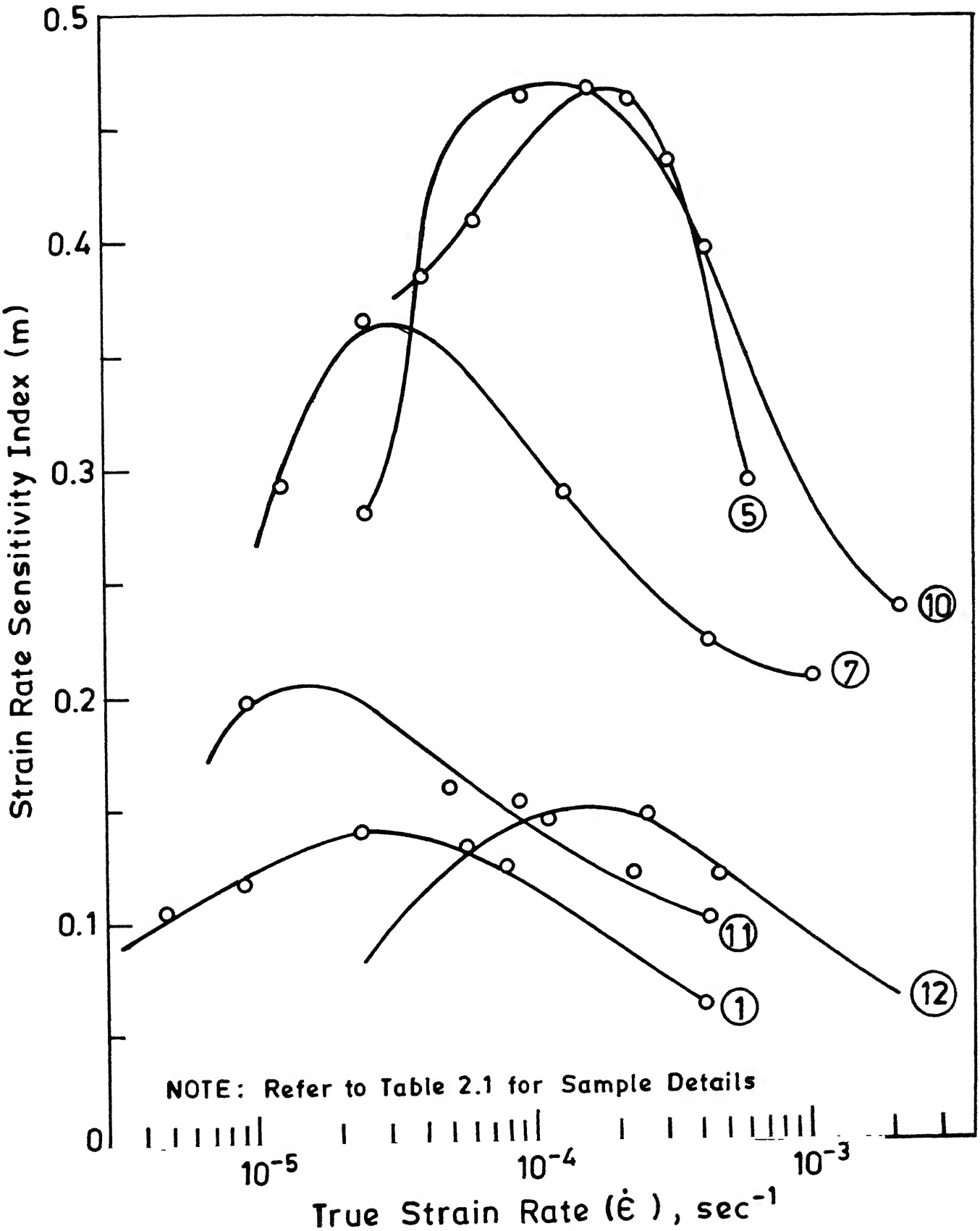

Fig.3.9 Strain rate sensitivity index vs true strain rate plots for different treatments.

3.3 Strain Rate Sensitivity (m) - Strain Rate ($\dot{\varepsilon}$) Behaviour

In Figure 3.9 plots of m versus $\dot{\varepsilon}$ are presented for the samples treated differently. In all the cases, m is low at low and high strain rates and exhibit a maximum at intermediate strain rates. There are two distinct features noticeable from these plots, namely: (i) the peak 'm' values occur at different strain rate levels and (ii) the range of 'm' values differ, from treatment to treatment. From the data presented it is noticed that there are two distinct groups of samples (I) those that have low peak 'm' values and (II) those that have high peak 'm' values. The first group of samples showing low peak 'm' values are

a. Cold worked and annealed
b. Thermally cycled
c. Hot iso rolled in the austenite range

The second group of samples, showing high peak 'm' values are:

d. Hot-continuously rolled
e. Hot-iso rolled at lower temperature
f. Single quenched and hot iso rolled.

In group I samples, the range of 'm' spans from values < 0.1 to values < 0.2 whereas in group II, 'm' ranges from values ≥ 0.1 to values > 0.4 upto 0.46. Table 3.1 gives the values of peak 'm', $\dot{\varepsilon}$ ranges for various samples.

3.4 Effect of Repeated Strain Rate Cycling on $\sigma - \dot{\varepsilon}$ Behaviour

To assess the steady state flow behaviour during deformation repeated strain rate cycling tests were done for

Table 3.1

Summary of Results

	Treatment	Sample No.	Maximum 'm' value	Strain rate at maximum 'm' value (sec^{-1})
I	Hot isorolling process	1	0.199	2.63×10^{-5}
		2	0.460	1.58×10^{-4}
II	Hot continuous rolling	3	0.369	1.15×10^{-4}
		4	0.372	1.10×10^{-4}
		5	0.464	1.55×10^{-4}
III	Single quench and isorolling	6	0.456	6.12×10^{-5}
		7	0.429	3.09×10^{-5}
		8	0.426	1.55×10^{-5}
		9	0.451	6.08×10^{-5}
		10	0.469	4.64×10^{-5}
IV	Thermal cycling	11	0.207	2.97×10^{-5}
V	Cold rolling and annealing	12	0.254	2.57×10^{-5}

Refer to Table 2.1 for more details of the samples.

samples treated differently. The results are shown in Figures 3.10 to 3.14.

Two distinct types of behaviour is observed corresponding the two groups of samples. Group I samples show no change in flow stress though repeated strain rate cycling. However, group II samples show a change in flow stress in regions I and II. The flow stress is increased for each cycle from first through third though the change in flow stress level is large for cycle I to cycle II, the change is little for cycles II to III. Region III of these samples shows no change in flow stress through repeated strain rate cycling.

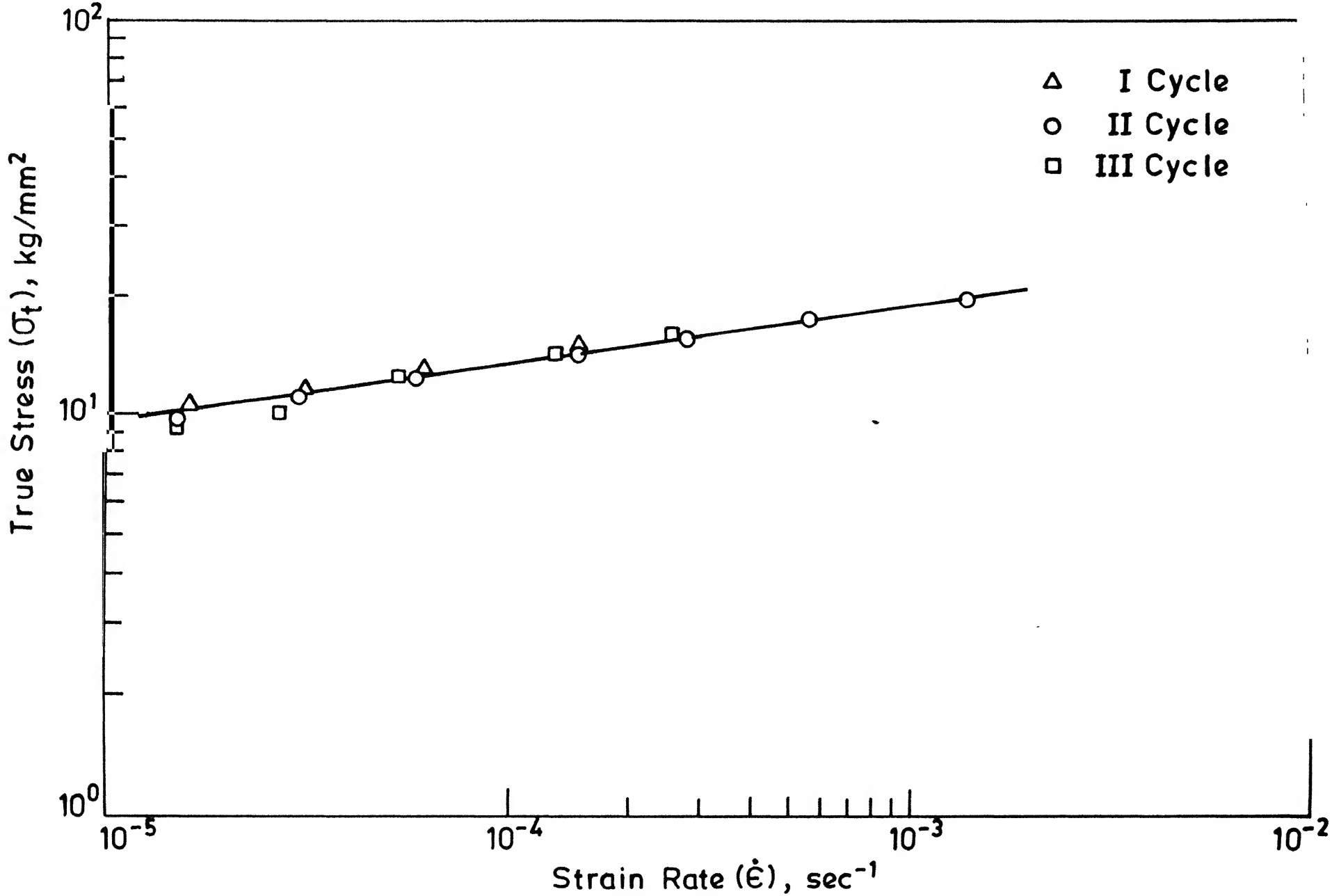

Fig. 3.10 Effect of repeated cycling on stress strain rate behaviour for therm-

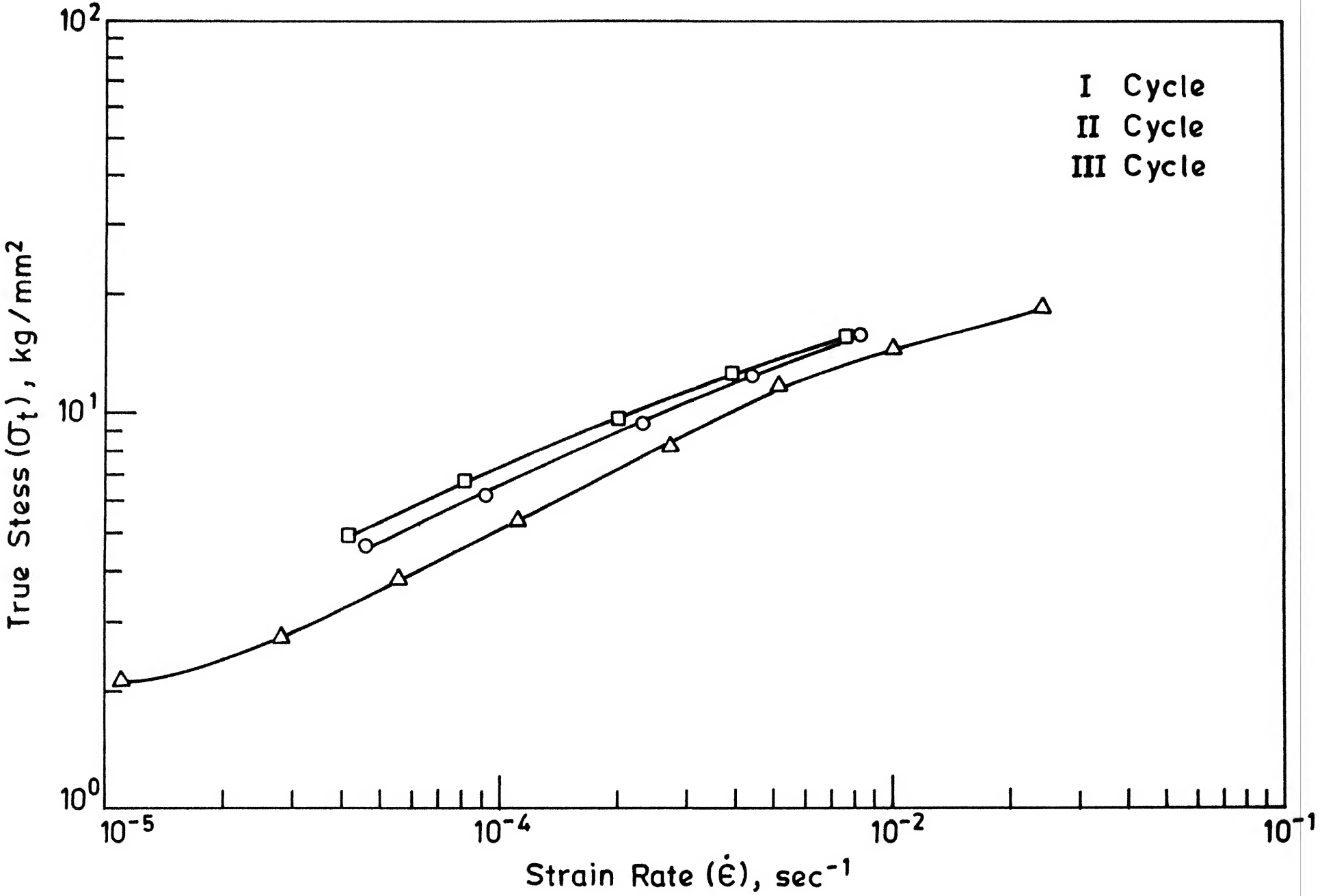

Fig. 3.12 Effect of repeated cycling on stress strain rate behavior for single quench and isorolled sample (#10)

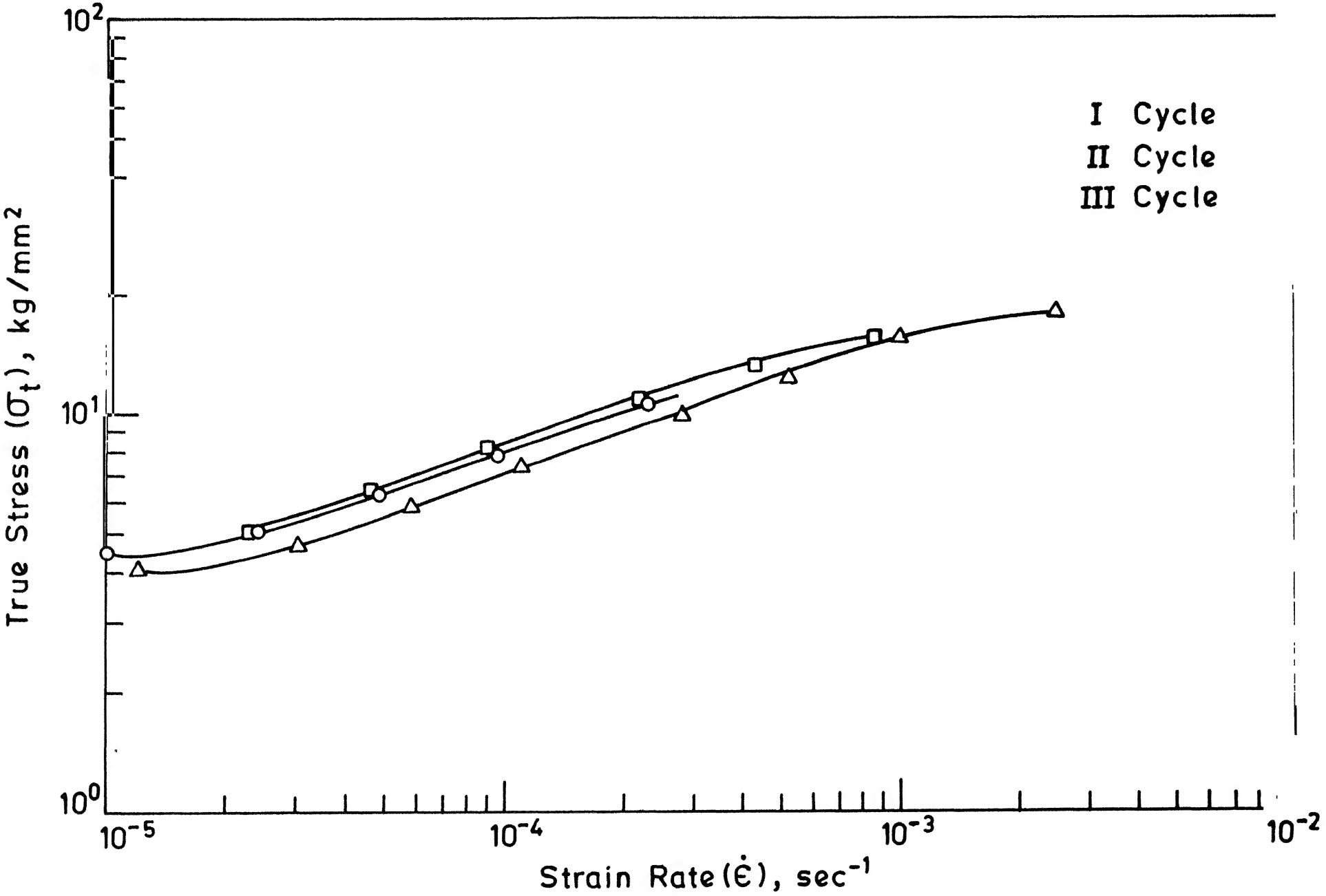

Fig. 3.13 Effect of repeated cycling on stress strain rate behaviour for hot continuously rolled sample (#3).

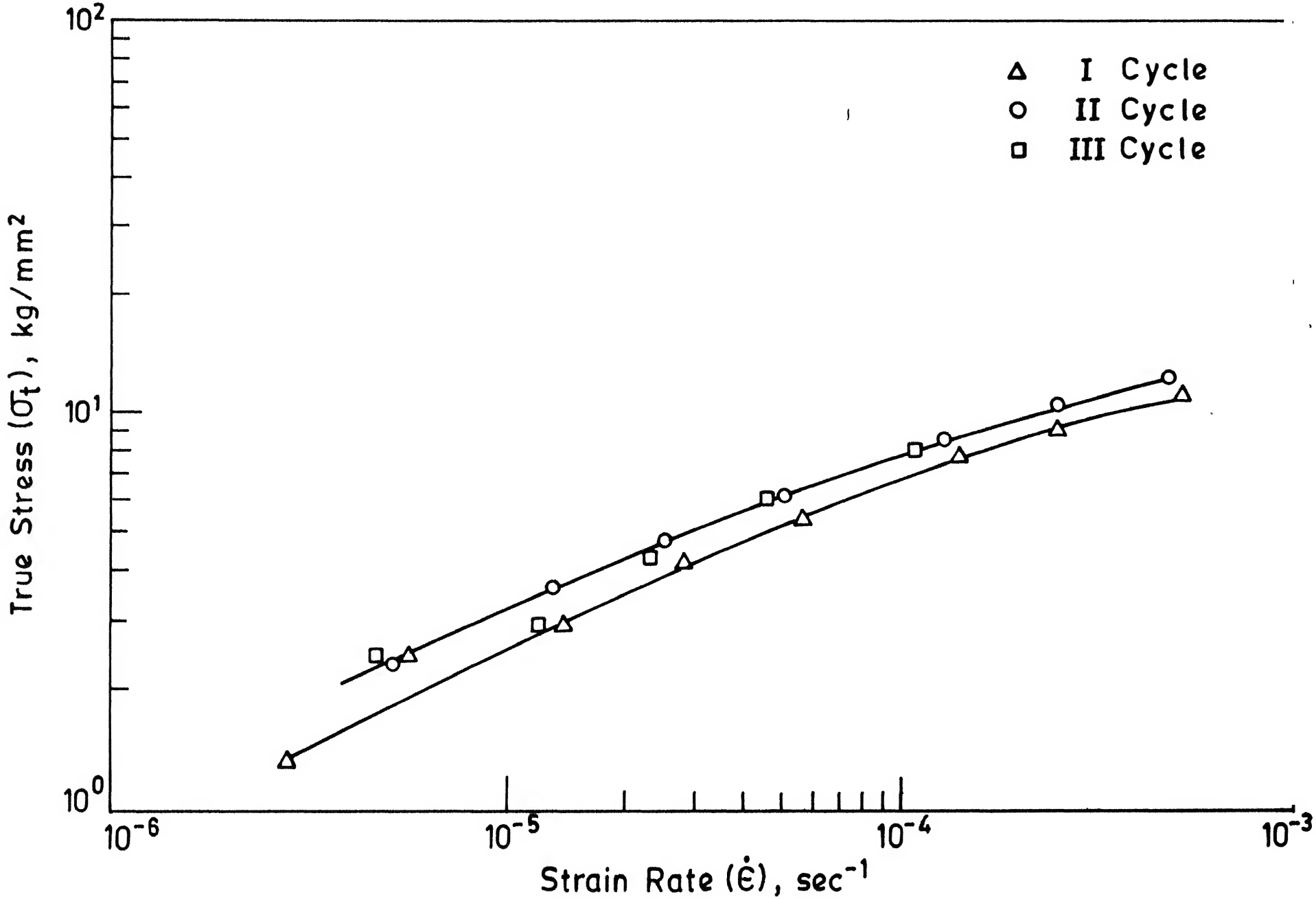

Fig. 3.11 Effect of repeated cycling on stress strain behaviour for hot continuously rolled sample (#5)

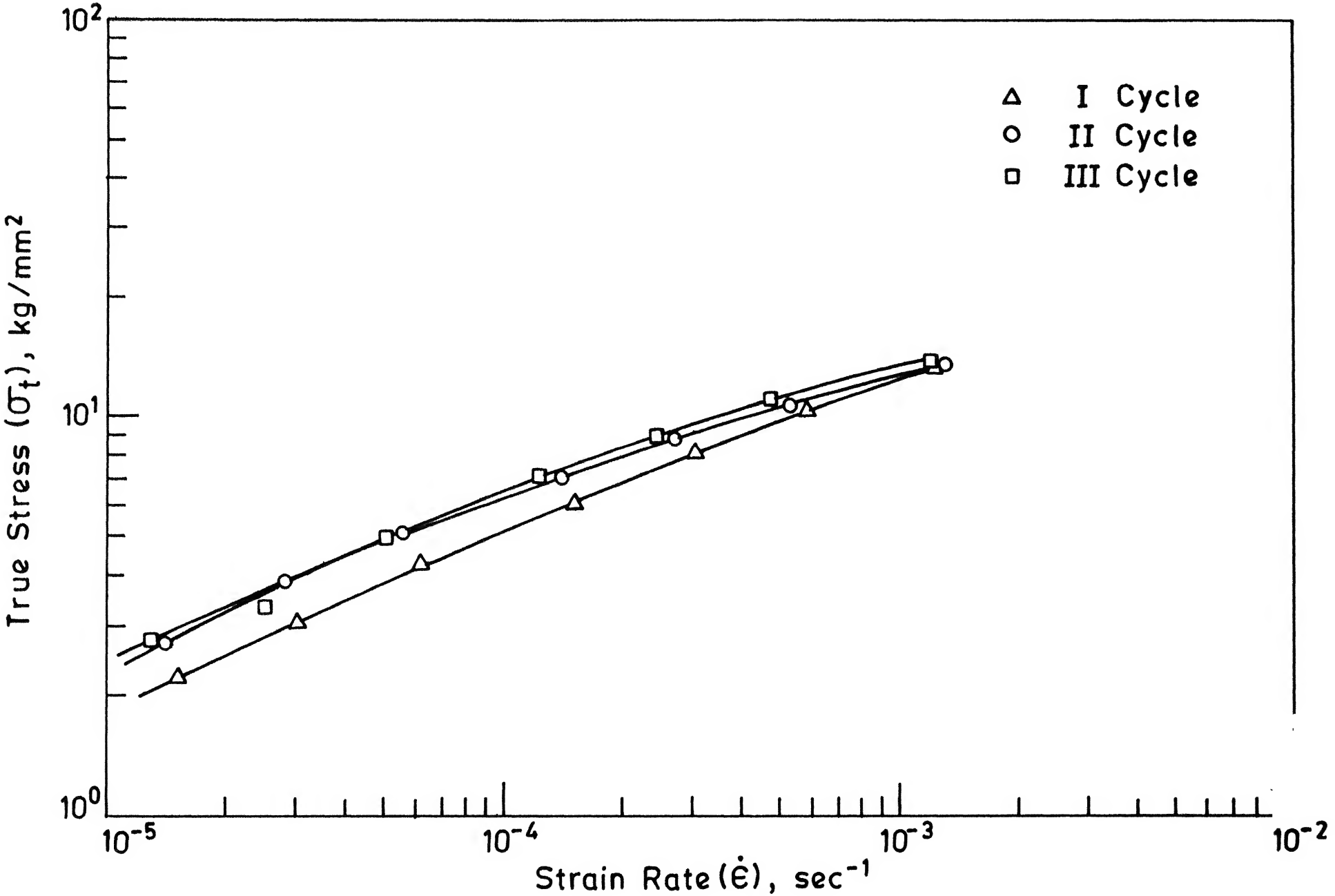

Fig. 3.14 Effect of repeated cycling on stress strain behaviour for water quench and isorolled sample (#7).

Chapter IV

Discussions

The results presented in Chapter III are explained below. The discussion follows the same sequence as that of the results.

4.1 Microstructures

The material in its as received condition is coarse grained with a thick cementite network at the grain boundaries. The eutectoid carbide is in a lamellar form. It is a normal structure expected in a steel containing carbon >0.8%.

Repeated thermal cycling treatment does refine the microstructure. In this treatment due to repeated, Austenite ⇄ Cementite, transformation the matrix grain size is expected to be refined considerable. Grain boundary cementite precipitation is avoided due to faster cooling during eutectoid reaction stage, viz., Austenite → Ferrite + Cementite transformation. However the eutectoid cementite is only partially spheroidised contrary to the expectations.

Cold working followed by anneal does lead to grain size reduction. However there is limit to the grain refinement by this process and the cementite, though globularised still remains coarse. Cementite cannot be finely divided by the treatment. On the contrary hot working is able to plastically deform cementite and thereby divide the cementite in an

extremely fine globularised structure. Concurrent recrystallization process is able to refine the grain size considerably. The lamellar morphology is effectively broken and the plastic deformation is able to disperse the phases more effectively.

The difference in structural refinement achieved through hot continuous and hot iso-rolling is negligible provided the deformation is carried through $\gamma \rightarrow Fe_3C$ transformation. If the hot iso-rolling is carried out in the austenite range the advantage of concurrent transformation is lost. In hot continuous rolling one gets the advantage of concurrent phase transformations. However continuously rolled samples seem to develop some directionality in the structure. On the other hand hot iso-rolling causes no such directionality because of longer time available at high temperature for the recovery processes.

Single quench followed by iso-rolling combines the advantage of grain refinement through the transformation of the metastable martensite phase obtained by fast cooling (quenching) from the austenite phase. Deformation processing further refines the grain size.

From the practical stand point of view continuous hot working from austenite phase through $\gamma \rightarrow Fe_3C$ transformation and $\gamma \rightarrow \alpha + Fe_3C$ transformation is a much more convenient method of obtaining extremely fine grained and homogeneous structure. There is no cumbersome procedure of repeated heating as in hot iso-rolling process. It is easier to operate technologically.

4.2 Stress-Strain Rate Behaviour

All the samples have been tested at 610°C which is close to 0.5 T_m (where T_m is the melting point expressed in °K) of the steel used. At this temperature, material is expected to observe the following stress-strain rate relationship;

$$\sigma = K \dot{\varepsilon}^m$$

where σ is the flow stress, K is a material constant, $\dot{\varepsilon}$ is the applied strain rate and m is the strain-rate hardening index or strain rate sensitivity. Stress is expected to increase with the increasing strain rate. However, the slope of the curves, which is the rate of change of strain rate expressed here as d log σ/d log $\dot{\varepsilon}$, would depend on 'm' since;

$$\log \sigma = \log K + m \log \dot{\varepsilon}$$

The value of 'm' depends upon therate controlling deformation mechanism.

At higher temperatures ($T > 0.4\ T_m$) contribution to deformation are made through several independent processes, such as

(i) Dislocation motion (slip) within grains

(ii) Grain boundary sliding

(iii) Mass transport through grains by lattice diffusion (N-H creep)

(iv) Mass transport along grain boundaries (Coble creep).

The diffusional mechanisms, viz. N-H and Coble creep, give 'm' value of 1. The grain boundary sliding mechanism gives 'm' value of 0.5 and the dislocation slip mechanism(s)

values in the range of 0.1 to 0.3. Based on these theoretical considerations it would appear that at higher strain rate range where 'm' is <0.3 dislocation slip process is the rate controlling mechanism. At intermediate strain rate range grain boundary sliding appears to be the rate controlling mechanism. However at low strain rates dislocation slip process would appear to control the deformation. But for the slip process to be operative there is a need of a threshold stress. Therefore it is less likely to be a rate controlling mechanism at low strain rates which corresponds to low flow stress values.

4.3 Strain Rate Sensitivity (m) versus Strain Rate ($\dot{\varepsilon}$)

As pointed out earlier, 'm' depends upon the rate controlling mechanism. The mechanisms themselves are structure sensitive, that is, their contributions to flow depend upon the grain size, nature of grain boundaries, the strength of phases and their distribution. Matrix grain size (grain size of the phase which has the largest volume fraction in a given alloy) and the size of the dispersed phase have the greatest effect on 'm' values. When both are very small (~ 5 μm) peak 'm' values are very large.

In the present case, Group I samples possess relatively coarser grain size and/or coarser second phase particle. These samples have exhibited lower peak 'm' values. The Group II samples are distinctly fine grained and with five second phase particles, hence shown greater peak 'm' values.

4.4 Microstructural Instability

We observed in Chapter III that Group II samples show a change in flow stress in regions II and III through repeated strain rate cycling. This suggests that the flow is not steady state, which in turn implies that the microstructure is not stable during deformation. This can be understood from the fact that the group II samples show microstructural inhomogeneity such as directionality, non-uniform particle (cementite) size and distribution. In addition to this grain growth through to a limited extent may be present. The little change of flow stress from cycle II to cycle III is likely due to the fact that the microstructure is tending to a homogeneous one during deformation.

No change in flow stress in region III of these samples is obvious because of independence of flow stress on microstructure (grain size) in this region.

The group I samples show no change in flow stress during repeated strain rate cycling. This is because only region III is observed ($m < 0.30$) for these samples in the entire strain rate range investigated. The operative mechanism is dislocation creep which is independent of microstructure or grain size. Thus the observed behaviour for these samples is clearly understood.

4.5 Superplasticity

Tensile ductilities >300% can be obtained in those materials which show strain rate sensitives >0.3. In the present case the steel samples belonging to group II treatments

are expected to show superplasticity. On testing, the group II samples do exhibit ductilities >> 300%. However, due to machine limitations the samples could not be tested beyond 450%. Even after 450% elongation these samples did not fracture or develop sharp neck. However, the samples belonging to group I have shown elongations <200% (Figure 4.1 and 4.1b).

From the practical stand point of view the strain rates at which m > 0.3 has been obtained are still 3 orders of magnitude lower than those prevail in normal metal working operations such as rolling, forging etc. Even then group II treated samples would show considerable ductilities at high strain rates since the general range of 'm' values is higher than 0.3.

Amongst group II treatments itself, single quench followed by iso rolling treatment gives the most ideal microstructure for superplastic flow. Therefore it is the most ideal treatment in inducing superplasticity in this grade of steel.

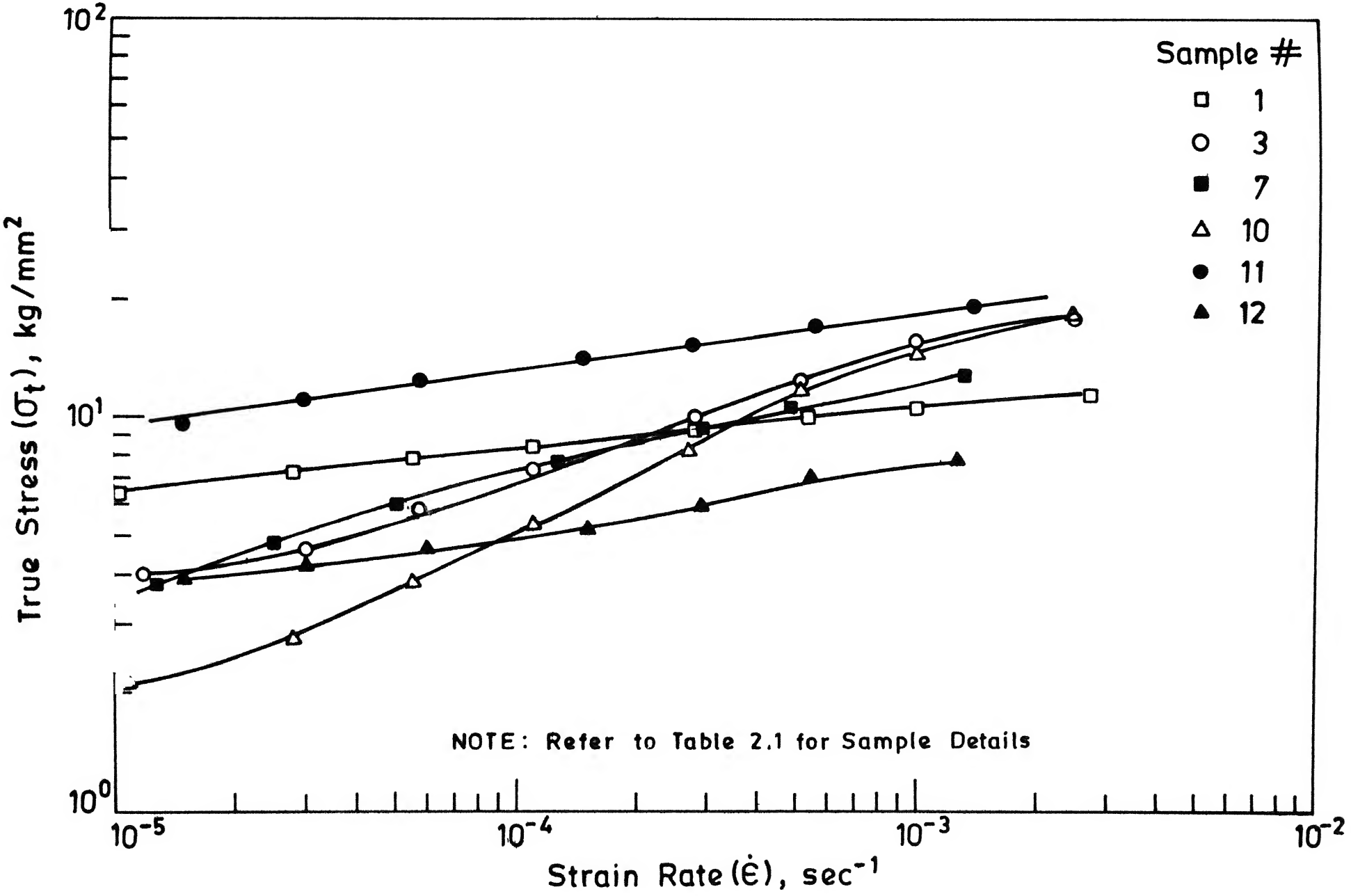

Fig.3.8 Stress strain rate relation ship for different treatments.

Chapter V

Conclusions

1. It is possible to obtain an extremely fine grained two phase microstructure in ultra high carbon steel containing 1.28% carbon by proper thermo-mechanical treatments.
2. Thermo-mechanically treated fine grained ultra high carbon steel exhibit a maximum strain rate sensitivity values close to 0.5 at 610°C and superplastic deformation >> 300%.
3. Amongst the various treatments, quenching from 940°C and iso-rolling at 730°C gives the most ideal microstructure suitable for superplastic effects.
4. From the practical stand point of view hot continuous rolling from austenite phase at 880°C to a temperature of 600°C through two phase transformation regions achieve microstructure which is quite adequate from the superplastic point of view.
5. Hot iso-rolling at the austenite temperature and cold working-annealing treatments are not suitable from the superplastic behaviour.

References

1. J. Wodsworth, T. Oyama and O.D. Sherby, Paper presented at the Sixth American Conference on Materials Technology (1980), page 32.

2.2. Bruno Walser and O.D. Sherby, The American Society for Metals and the Metallurgical Society of AMIE, Vol. 10A, October 1979, 1461.

3. Superplasticity by K.A. Padmanabhan and G.J. Davies, Springer-Verlag, Berlin, Heidelberg, New York (1980).

4. D. McLean, Deformations at High Temperatures, Met. Rev., 7, 481 (1962).

5. J.E. Bird, A.K. Mukerjee and J.E. Dorn, Correlations between High Temperature Creep Behaviour and Structure, Quantitative Relation between Properties and Microstructure, edited by D.G. Brandon and A. Rosen (Israel Univ. Press, Jerusalam), 255 (1965).

6. Backofen, W.A., Turner, I.R. and Avery, D.H., Trans. Am. Soc. Met. (57), (1964) 980.

7. Hedworth, J., Stowell, M.J., J. Mater. Sci., 6 (1971), 1061.

8. Murthy, G.S., "Stress Relaxation in Superplastic Materials", J. Mater. Sci., 8 (1973), 611.

9. Smith, C.I. and Ridley, N., Met. Technology, 1 (1974), 191.

10. Holt, D.L., Ultrafine Grain Metals (eds. Burke, J.J. and Weiss, V.), New York (1970), page 355.

11. Yoder, G.R. and Weiss, V., Metall. Trans., 3 (1972), 675.

12. Naziri, H. and Pearce, R.J., Inst. Met., 97 (1969), 326.

13. Biswas, C.R.D. and Murthy, G.S., Trans. Japan Inst. Met., 13 (1972), 8.

14. Stewart, M.J., Metall. Trans., 7A (1976), 399.

15. Reichman, S.H. and Sanythe, J.W., Int. J. Powder Met., 6(1), (1970), 65.

16. Porter, L.F. and Dabkowaski, D.S., "Grain Size Control by Thermal Cycling", Ultrafine-Grain Metals (Burke, J.J. and Weiss, V.), Conference Sagamore, New York, August (1969), pp. 133-161.

17. Grange, R.A., Trans. ASM, 59 (1966), 26-48,

18. Sherby, O.D., Walser, B., Young, C.M. and Cady, E.M., Scripta Met., 9 (1975), 569-574.

19. Walser, B. and O.D. Sherby, Met. Trans., 10A (1979), 1461-1471.

20. Hornbogen, E., Design of Heterogeneous Microstructures by Recrystallisation, pp. 389-410 in Jaffee,R. and Wilcox, B. (eds.), Fundamental Aspects of Structural Alloy Design, Plenum Press, New York (1977).

21. Mohamed, F.A., Ahmed, M.M.I. and Langdon, T.G., Phil. Mag., 32 (1975), 1443-1450.

22. Cottrell, P. and Mould, P.R., Recrystallisation and Grain Growth in Metals, Surrey University Press, London, 1976, pp. 181-249.

23. Langdon, T.G., "The Mechanical Properties of Superplastic Materials", Met. Trans., 13A (1982), 681.

24. Grifkins, R.C. and Langdon, T.G., "Comments on Theories of Structural Superplasticity", Mater. Sci. Engg., 36 (1978), 27.

25. Langdon, T.G., Current Problems in Superplasticity Creep and Fracture of Engineering Materials and Structures (B. Wilshire and D.R.J. Owen, eds.), Pincridge Press, Swansea, Wales (1981), 141.

26. Ashby, M.F. and Verall, R.A., "Diffusion Accommodated Flow and Superplasticity", Acta Met., 21 (1973), 149.

27. Ball, A. and Hutchison, M.M., Superplasticity in the Aluminium-Zinc Eutectoid", Metal. Sci. J., 3 (1969), 1.

28. Gifkins, R.C., "Grain Boundary Sliding and Its Accommodation During Creep and Superplasticity", Met. Trans., 7A (1976), 1225.

29. Gittus, J.H., Theory of Superplastic Flow in Two Phase Materials: Role of Interphase Boundary Dislocations Ledges and Diffusion, Trans. ASME, 99 (1977), 244.

30. Gittus, J.H., High Temperature Deformation of Two-Phase Structures", Phil. Trans. R. Soc. Lod., A288 (1978), 12.

31. Ashby, M.F., and Verall, R.A., "Diffusion Accommodated Flow and Superplasticity", Acta Met., 21 (1973), 149.

32. Padmanabhan, K.A., "A Theory of Structural Superplasticity", Mater. Sci. Eng., 29 (1977), 1.

33. K.e, T.S., "A Grain Boundary Model and the Mechanism of Viscous Intercrystalline Slip", J. Appl. Phys., 20 (1949), 274.

Date Slip

This book is to be returned on the date last stamped.
